2006 LAB NOTES

EDITORS
Thomas M. Moses
Shane F. McClure
GIA Laboratory

Lizards in IMITATION AMBER

As the saying goes, "When it rains, it pours." In this case, it's pouring lizards. Recently, not one but two items resembling lizards trapped in amber were submitted to the West Coast laboratory for identification reports (figure 1). Although we occasionally see specimens with insects or animals enclosed in amber or amber imitations (i.e., plastic or copal), it is unusual to have two such pieces submitted within days of each other. Having both samples in the laboratory at the same time offered a special opportunity to examine the similarities and differences between two potentially rare specimens.

The first sample (58.14 × 35.75 × 24.41 mm; figure 1, left) contained a badly decomposed lizard with a broken tail and one foot missing. Microscopic examination between crossed polarizers revealed a narrow strain zone surrounding the lizard's body. Gas bubbles and bits of fiber were also present, but these were inconclusive for determining whether the host material was amber, copal, or plastic. A spot refractive index (R.I.) reading of 1.55 was obtained—a bit high for amber, but still inconclusive. The fluorescence was chalky greenish yellow to both long- and short-wave ultraviolet (UV) radiation, which was also not conclusive. The hydrostatic specific gravity (S.G.) was ~1.18. For confirmation, the piece was placed in a saturated saline solution (S.G. = 1.13). It was observed to sink at a rate that was consistent with an S.G. of ~1.18–1.20. However, since the presence of the lizard would affect the S.G. of the specimen, further testing was necessary.

The separation of amber from plastic or copal is gemologically challenging, because the easiest and most reliable tests are destructive. Therefore, we decided first to analyze the sample with our Raman system using excitation from a 785 nm diode laser. The 785 nm laser is useful because it eliminates many problems related to sample fluorescence. The resulting Raman spectrum (figure 2) indicated that the specimen was neither amber nor copal, but rather a polystyrene plastic. All the gemological properties reported above were consistent with polystyrene. After consultation with

Figure 1. These two specimens proved to be imitations of amber with lizards enclosed. On the left, the lizard was encased in polystyrene; the sample on the right was an assembled piece consisting of a copal base, a plastic top, and a lizard molded between them.

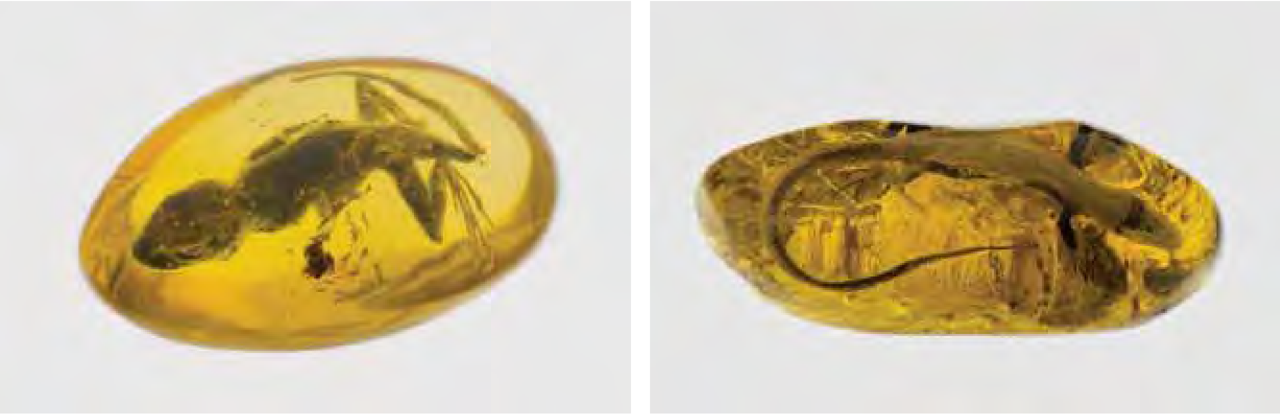

the client, we tested a small area with a hot point: The acrid odor confirmed our identification.

The second sample (74.5 × 31.9 × 25.32 mm; figure 1, right) was more easily identified than the first. The lizard was in much better condition, having undergone markedly less decomposition. Using magnification and reflected light, we saw a separation plane between the part of the sample below the lizard and the part above, clearly indicating that the specimen had been assembled. Microscopic observation also revealed numerous gas bubbles concentrated along this separation plane. The base of the specimen contained clouds, fractures, and various particles, whereas the upper portion showed a wide strain pattern, flow lines, and gas bubbles around the lizard's body. The R.I. was 1.54 for the lower portion and 1.57 for the upper part. Both halves showed chalky greenish yellow to yellow UV fluorescence, but the lower half showed slightly stronger fluorescence when exposed to long-wave UV.

When the second sample was immersed in the saturated saline solution, it floated with the base up, suggesting an S.G. of ~1.10 for that portion—enough to flip the piece over, but not to sink it. The base had been left rough and pitted, providing a surface on which to conduct hot point and acetone tests where small blemishes would not be noticeable. When the pitted surface was exposed to heat, the odor was resinous and consistent with either amber or copal. Application of acetone to a small area of the base softened the material and left the area slightly etched, a reaction consistent with copal (amber would not be affected). Both the top and bottom parts were analyzed using the 785 nm Raman system for comparison to the first sample. The spectrum for the lower half of the piece indicated amber or copal, whereas the spectrum from the upper half did not match amber, copal, or polystyrene. The R.I., S.G., Raman spectrum, and microscopic features were consistent with a plastic top, but not with polystyrene specifically. Thus, our final conclusion was that this second piece was an assembled specimen consisting of a copal base, a plastic top, and a lizard molded between.

These two items illustrate some of the means and materials that can be used to create imitations of creatures preserved in amber (see the Winter 2005 Gem News International, pp. 361–362, for yet another example). These circumstances also illustrate the ongoing quest of gemological laboratories to develop new and effective nondestructive testing methods to supplement or replace traditional destructive tests.

Kimberly Rockwell

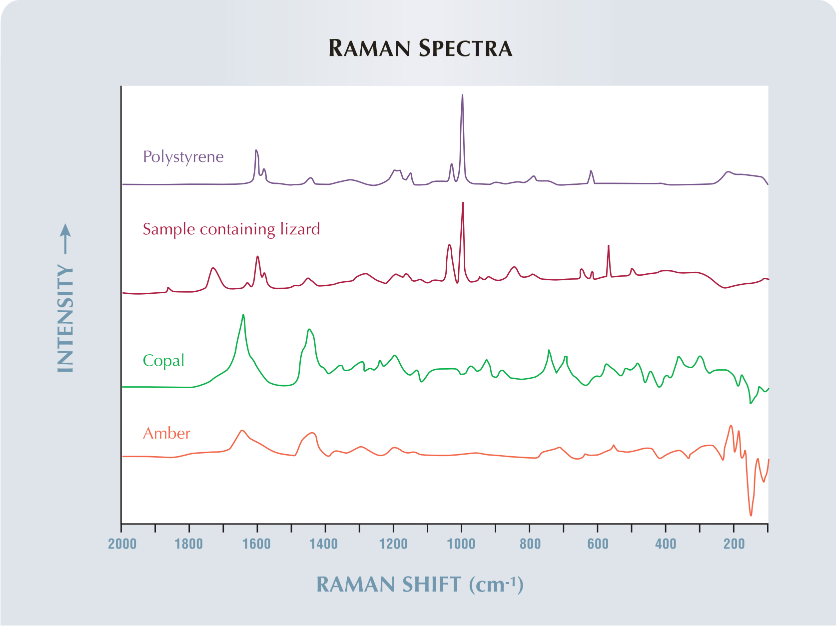

Figure 2. Raman spectroscopy (785 nm excitation) was effective in identifying the material encasing the lizard in figure 1 (left) as polystyrene. Note, however, that the spectra of amber and copal are too similar for this technique to conclusively separate those two materials.

Editor's note: All items are written by staff members of the GIA Laboratory, East Coast (New York City) and West Coast (Carlsbad, California).

GEMS & GEMOLOGY, Vol. 42, No. 4, pp. 260–267

Large DEMANTOID of Exceptional Color

Recently, the East Coast laboratory received the 5.82 ct transparent green round-brilliant-cut stone in figure 3 for identification. Standard gemological properties (R.I. = OTL, singly

Figure 3. This 5.82 ct demantoid garnet is notable for its exceptional color and size, as well as its unusual pattern of inclusions.

Figure 4. The demantoid in figure 3 contained striking inclusions composed of randomly oriented curved fibers encircled by small, bright, disc-like features. Magnified 50×.

refractive, moderate dispersion, S.G. = 3.84, and chrome lines and a 470 nm cutoff seen with the desk-model spectroscope) identified the gem as a demantoid garnet.

The classic Russian demantoids are famous for their easily observed "horsetail" inclusions—golden yellow curved needles radiating from a point like the tail of a horse. These needles were originally believed to be the asbestiform amphibole byssolite but more recently have been identified as chrysotile (see W. R. Phillips and A. S. Talantsev, "Russian demantoid, czar of the garnet family," Summer 1996 *Gems & Gemology*, pp. 100–111; M. O'Donoghue, *Gems*, Butterworth-Heinemann, Oxford, England, 2006, p. 209). Microscopic examination of this stone revealed needles in a random orientation, as has been observed in some demantoids from a few of the newer Russian localities. Also present were bright disc-like inclusions along the curved needles (figure 4), which gave the inclusion scene an exotic appearance.

The combination of the stone's relatively large size and strong color saturation was also unusual, as most fine demantoids are less than one carat or, if larger, often have more yellow in the bodycolor. The owner of the stone, Isaac Aharoni of Isaac Aharoni Inc., New York, reported that he purchased it in Russia. This was the second large demantoid garnet we have seen recently, as we also identified a 3.20 ct demantoid for Mr. Aharoni.

Wendi M. Mayerson

DIAMOND

Unusually Large Fancy White Diamond with Whitish Banding

Diamonds occasionally contain submicroscopic inclusions, which usually induce a brownish or grayish color appearance and can have a negative impact on clarity. In rare cases, these tiny inclusions can produce a translucent milky "white" color by scattering light that passes through the stone (see E. Fritsch and K. Scarratt, "Gemmological properties of type Ia diamonds with an unusually high hydrogen content," *Journal of Gemmology*, Vol. 23, No. 8, 1993, pp. 451–460; Summer 2000 Lab Notes, p. 156; and the article by J. M. King et al. on pp. 206–220 of this issue). Such was the case with the unusually large (30.87 ct) diamond in figure 5, which was recently examined by the East Coast laboratory.

This Fancy white pear modified brilliant measured 27.96 × 15.91 × 11.53 mm and was submitted for a Colored Diamond Identification and Origin Report. The diamond fluoresced strong blue to long-wave UV radiation and moderate-to-strong blue to short-wave UV. When the short-wave UV lamp was turned off, it phosphoresced weak blue for more than 30 seconds. No absorption lines were visible with a desk-model spectroscope, and the absorption spectrum in the mid-infrared region revealed that it was a nearly pure type IaB diamond with a very high concentration of nitrogen. These properties, except for the unusual phosphorescence, are typical for type IaB Fancy white diamonds (again, see the Summer 2000 Lab Note). Strong absorption peaks were also present at 3105 and 1405 cm^{-1}, caused by structurally bonded hydrogen, a common feature of cloud-bearing diamonds (again, see Fritsch and Scarratt, 1993).

In addition to its size, an unusual feature of this diamond was the occurrence of straight whitish banding observed throughout the entire stone (figure 6). In the overwhelming majority of instances, whitish graining caused by submicroscopic inclusions is part of the growth structure and results in a homogenous, milky appearance. The strong banding of the submicroscopic inclusions, which is undoubtedly the cause of the white coloration, is something we have only rarely observed in other type IaB Fancy white diamonds (see Spring

Figure 5. The color of this 30.87 ct Fancy white diamond is due to milky bands of submicroscopic inclusions. Also present are numerous partially graphitized stress fractures.

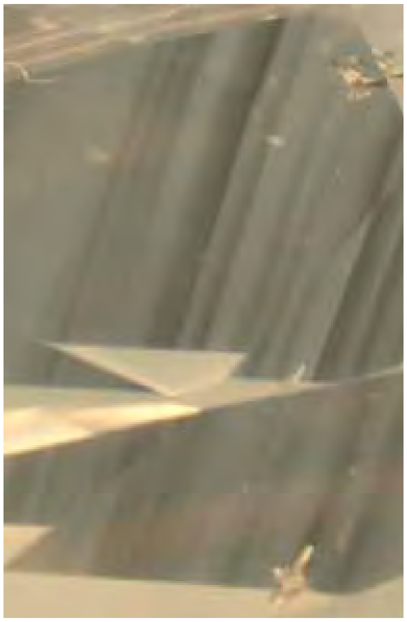

Figure 6. The submicroscopic inclusions in the diamond in figure 5 are concentrated in bands, something that is rarely seen in Fancy white diamonds. Magnified 15×.

1992 Gem News, p. 58). Also visible internally were many rounded crystals, surrounded by partially graphitized stress fractures (again, see figures 5 and 6). However, it is the large size and the unusual color and banding throughout the stone that make this diamond special.

HyeJin Jang-Green

Prolonged Change of Color in Pink Diamond

Change of color in diamonds occurs most frequently in "chameleon" diamonds, which are predominantly greenish yellow to yellowish green in ambient conditions but change to predominantly brownish or orangy yellow after gentle heating or prolonged storage in the dark. In rare instances, however, some diamonds have been known to change color temporarily when cryogenically cooled or exposed to ultraviolet radiation.

The East Coast laboratory recently received a 0.84 ct pink diamond for color grading. As is typical of type Ia pink diamonds, it exhibited obvious pink graining and moderate green transmission luminescence when viewed with magnification. It fluoresced strong blue to long-wave UV radiation and weaker blue to short-wave UV. The exposure to UV radiation resulted in an obvious change in apparent color from Fancy Deep pink to Fancy Deep orangy pink (figure 7; we were not able to determine whether the change resulted from long- or short-wave UV).

Although the lab has reported on a few similar stones in recent years (see Summer 2002 Lab Notes, pp. 165–166; Winter 2005 Lab Notes, pp. 342–344), the color change has always been temporary, with the diamond reverting to its stable color in a matter of a few seconds to a few hours in normal lighting. Thus, we were surprised to see that this particular diamond retained its orangy pink color for approximately two weeks.

Mindful of the time constraints on lab report services, we attempted to accelerate the return of the pink stable color state. Gentle heating with an alcohol flame, the technique typically used to induce a color change in chameleon diamonds, had no apparent effect. We then cooled the diamond by immersing it in liquid nitrogen, which produced a minimal color shift toward pink. Repeated immersions—or perhaps simply the passage of time—eventually restored the original deep pink color.

Figure 7. The 0.84 ct Fancy Deep pink diamond on the left changed to Fancy Deep orangy pink after exposure to UV radiation (right). Unlike similar diamonds seen by the lab in the past, this change of color persisted for about two weeks.

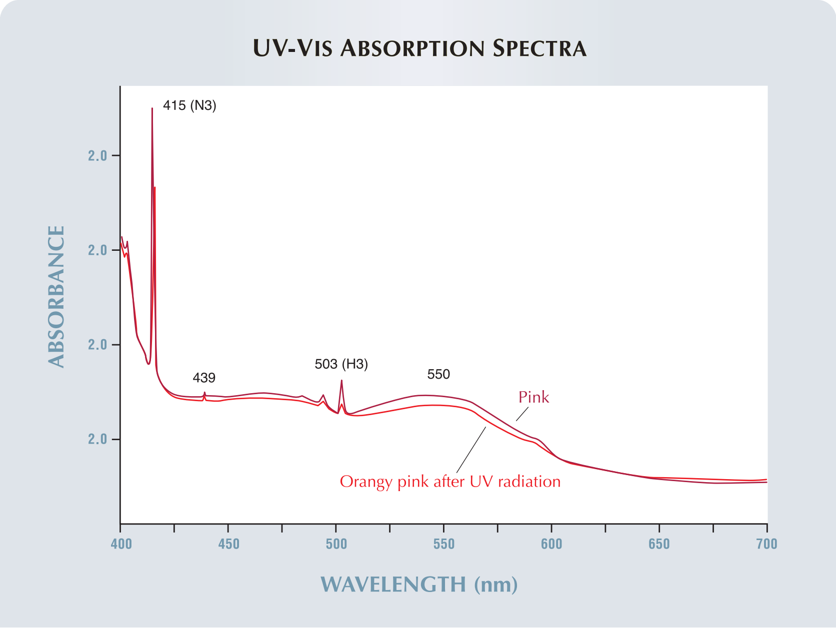

Figure 8. UV-Vis spectroscopy performed on the diamond in figure 7 in both stable and unstable color states showed a decrease in the 550 nm band that is responsible for the pink color of natural pink diamonds.

UV-visible spectroscopy performed during both color states showed the broad band at 550 nm that is typically responsible for natural pink color (figure 8; also see the Winter 2005 Lab Note). Exposure to UV radiation caused a decrease in the intensity of this band, resulting in a transmission window in the orange region and an apparent orangy pink color in the diamond. However, we were not able to determine why the orangy pink color had such a prolonged duration.

It was later suggested by the client that moderate heating of this diamond might result in a shift toward purple, as it had "turned purple" during recutting. Under nonlaboratory conditions in the client's office and with the client's assistance, we were able to heat the diamond using an electric coil hot plate. Although an accurate fancy-color grade could not be established without using the lab's standard viewing environment and procedures, we were indeed able to discern a shift toward purplish pink. This change of color, however, lasted only a few minutes. Advanced testing was not possible off site, so we could not obtain comparable UV-Vis spectral data.

Although change of color in diamond as a result of exposure to UV radiation is not a new phenomenon, this stone's two-week sustained change is particularly noteworthy.

Siau Fung Yeung and Wuyi Wang

Strand of Natural Nacreous and Non-nacreous PEARLS

The East Coast laboratory recently received for identification a graduated strand of 105 round to near-round colored pearls ranging from 2.35 to 5.90 mm (figure 9). From their worn condition, all appeared to be fairly old.

Most of the pearls in the strand were non-nacreous and a variegated brown (often modified by orange, red, or purple) in color. These pearls were somewhat worn, and a number of them had a dried-out appearance; some were cracked or even broken. As explained in a Fall 2005 Gem News International entry (p. 267),

Figure 9. This unusual strand proved to be comprised of non-nacreous pen shell and clam pearls, as well as natural saltwater pearls.

Figure 10. With 90× magnification, the columnar crystalline growth structure of one of the pen shell pearls is visible on this broken surface.

such deterioration is typical of the non-nacreous pearls from pen shell mollusks. The surfaces of these pearls also showed an unusual interlocking crystalline pattern similar to that seen on the non-nacreous pen shell products (E. Strack, *Pearls*, Ruhle-Diebner-Verlag, Stuttgart, Germany, 2006).

Spaced between the brown non-nacreous pearls were eight other porcelaneous pearls ranging from white to yellowish orange and pink, which exhibited varying degrees of color saturation and flame structure. Based on their distinctive structure, these appeared to be giant clam pearls from *Tridacna gigas*.

Finally, there were six white-to-"cream" colored nacreous pearls. These pearls exhibited good luster, various overtone colors, and a platelet-layered nacre structure, all characteristics consistent with natural saltwater pearls.

An X-radiograph revealed natural growth structures in all the pearls. The pen shell pearls displayed a columnar crystalline growth structure, which was also visible with magnification where one was broken (figure 10), while the clam pearls and nacreous pearls revealed either no visible structure or a layered concentric growth structure typical of those pearl types.

Exposure to long-wave UV radiation produced varied reactions. The pen shell pearls displayed fluorescence ranging from weak-to-strong chalky red and orangy red. The clam pearls displayed moderate pink and yellow fluorescence with some chalkiness as well. The nacreous pearls displayed no fluorescence when exposed to X-rays. Each of these reactions was consistent with the apparent pearl type.

It is quite uncommon to see a strand composed of a combination of natural nacreous and non-nacreous pearls from three different types of mollusks, and this proved an interesting identification exercise.

Akira Hyatt

[Editors' note: Though past G&G *and GIA Laboratory style has been to place quotation marks around the word* pearl *when referring to non-nacreous pearls, the decision has been made to discontinue this practice.]*

POUDRETTEITE

The East Coast laboratory received a 3.90 ct transparent light purplish pink pear mixed cut for identification (figure 11). Standard gemological properties showed it to be a doubly refractive uniaxial gemstone with refractive indices of 1.515–1.535 and a hydrostatic S.G. of 2.50. Microscopic examination revealed needle-like growth/etch tubes of varying thickness, many with orange-yellow epigenetic staining; some "fingerprints" showed similar staining (figure 11, right). A two-phase (liquid-gas) inclusion was also present. The stone showed moderate pinkish purple and blue-green pleochroism. It was inert to long-wave UV radiation, but showed a very weak yellow reaction to short-wave. These properties were not a match to any gemstone found in the GIA Lab Manual, so we turned to more advanced testing. Raman spectroscopy confirmed that the stone was a faceted example of the mineral poudretteite.

Discovered in the mid-1960s, but not recognized as a new mineral by the International Mineralogical Association until 1986 (C. P. Smith et al., "Poudretteite: A rare gem species from the Mogok Valley," Spring 2003 *Gems*

Figure 11. This 3.90 ct poudretteite (9.45 × 10.04 × 6.58 mm) is the first ever submitted to the GIA lab (face-up, left). Eye-visible orange-yellow epigenetic staining is present in both "fingerprints" and needle-like growth/etch tubes (pavilion up, right).

& Gemology, pp. 24–31), poudretteite is extremely rare. The first seven crystals, named after the family who owned and operated the quarry in Mont Saint-Hilaire, Quebec, where they were found, were quite small—the longest measured just 5 mm. A comprehensive study of a 3.00 ct poudretteite purchased in Myanmar's Mogok Valley in 2000 was published in the Spring 2003 *Gems & Gemology* (again, see Smith et al.). The properties of the stone we examined were consistent with those described by Smith et al. This is the first poudretteite submitted to the GIA Laboratory for an identification report.

Wendi M. Mayerson

Unusual Gem PYROXMANGITE

Pyroxmangite is another gem material for which basic gemological techniques are inadequate to assign a specific identification. It is difficult to distinguish from other similar minerals, in particular rhodonite, without advanced techniques. Pyroxmangite usually forms in metamorphosed manganese ore deposits and other manganese-rich rocks and minerals. It is found in Japan; Broken Hill, New South Wales, Australia; Minas Gerais, Brazil; and Colorado, among other localities. It is usually closely associated with rhodonite (J. W. Anthony et al., *Handbook of Mineralogy*, Vol. 2, Mineral Data Publishing, Tucson, Arizona, 2003). Because it is typically massive and polycrystalline, and it may be intergrown with rhodonite, facet-quality material is rare.

The East Coast laboratory recently received one faceted specimen, a transparent red 0.68 ct modified lozenge step cut measuring 6.53 × 4.87 × 3.07 mm (figure 12). It had refractive indices ranging from 1.728 to 1.743, with strong purplish red to strong orangy red pleochroism and an S.G. of 3.71. Examination with a microscope using up to 60× magnification revealed large two-phase inclusions and whitish tubules containing a dark gray to black material. Two directions of cleavage were visible at the surface along with a few cavities, and the stone took only a moderate polish. With a desk-model spectroscope, we observed a strong band at 410–420 nm, a sharp line at 503 nm, and a broad band at 540–560 nm, indicative of a high manganese content.

Figure 12. This 0.68 ct modified lozenge step cut proved to be a rare faceted example of pyroxmangite.

We were able to measure the refractive indices and specific gravity with enough precision to narrow the possible identification to either pyroxmangite or rhodonite (table 1). Unfortunately, chemical and spectroscopic analyses are not useful in separating these two minerals, because their chemical compositions and spectral characteristics are so similar. Both belong to a group of minerals called $(Ca,Mn)SiO_3$ pyroxenoids. These pyroxenoids (which include rhodonite, ferrosilite III, wollastonite, bustamite, and the pyroxmangite-pyroxferroite series) are part of a larger group of minerals called chain silicates, because their basic structure comprises chains of silica tetrahedra (SiO_4). Differing amounts of Ca, Mn, Mg, and Fe result in different minerals with slightly different chain lengths, and these slight variations in crystal structure allow the separation of pyroxmangite from rhodonite using a technique developed in the early 20th century, powder X-ray diffraction (XRD) analysis.

Powder X-ray diffraction can distinguish two minerals with very similar crystal structures by determining

TABLE 1. Properties of rhodonite and pyroxmangite.[a]

Property	Rhodonite	Pyroxmangite
Formula	$(Mn,Fe,Mg,Ca)SiO_3$	$MnSiO_3$[b]
Refractive indices		
α	1.711–1.734	1.728–1.748
β	1.716–1.739	1.730–1.742
γ	1.724–1.748	1.746–1.758
Optic character	Biaxial positive	Biaxial positive
Color	Pink, red, gray, yellow	Pink, red
Pleochroism	Yellowish red, pinkish red, pale yellowish red	Moderate red, purplish red, orangy red
Specific gravity	3.57–3.76	3.61–3.80
No. of SiO_4 per unit cell	5	7
XRD pattern		
Spacing in Å (Intensity)	2.772 (100)	2.967 (100)
	2.980 (65)	2.188 (45)
	2.924 (65)	4.73 (35)
	3.14 (30)	2.630 (35)
	3.34 (25)	1.422 (30)
	3.10 (25)	3.47 (25)
	2.651 (18)	3.04 (25)

[a] *From J. W. Anthony et al.,* Handbook of Mineralogy, *Vol. 2, Mineral Data Publishing, Tucson, Arizona, 2003). Note: Because pyroxmangite cannot be separated from rhodonite using gemological properties alone, X-ray diffraction analysis was used to compare the crystal structure of each mineral.*

[b] *Pyroxmangite frequently also contains iron, because it forms a series with pyroxferroite $(Fe,Mn,Ca)SiO_3$.*

the spacing and angles between the atomic planes of the crystal structure. For analysis, a very small amount of material is scraped from the girdle of a faceted stone or the base of a cabochon. X-rays are transmitted through this powdered sample, and some of the X-rays are diffracted by the crystal structure to cast a characteristic pattern of arcs on photographic film or digital imaging equipment. The pattern for an unknown sample is then compared with a library of patterns of known materials.

Comparing the XRD pattern of the submitted stone with reference patterns of pyroxmangite (with a seven-silica tetrahedral chain) and rhodonite (with a five-silica tetrahedral chain) indicated that the submitted stone had a crystal structure with a seven-silica tetrahedral chain and atomic spacing consistent with pyroxmangite (table 1).

This rare faceted pyroxmangite is a prime example of a gem that requires advanced techniques in conjunction with good gemological testing to distinguish it from other similar minerals.

Carolyn van der Bogert
and Dino DeGhionno

PHOTO CREDITS
C. D. Mengason—1; Elizabeth Schrader—3, 9, and 11; Wendi Mayerson—4; Jessica Arditi—5, 7, and 12; HyeJin Jang-Green and Siau Fung Yeung—6; Akira Hyatt—10.